The interpretation of pyrrhotine–pentlandite–tochilinite–magnetite–magnesite textures in serpentinites from Mount Keith, Western Australia

R. VAN DE VUSSE*

Department of Geology, University of Western Australia, Nedlands, Western Australia, 6009, Australia

AND

ROGER POWELL

Department of Earth Sciences, University of Leeds, Leeds LS2 9JT, UK

ABSTRACT. The ultramafic-hosted disseminated nickel sulphide deposit at Mount Keith, Western Australia, originally consisted of sulphide droplets and chrome spinels interstitial to olivine. During cooling, the sulphide droplets crystallized to pentlandite–pyrrhotine. Hydration and carbonation caused rimming and replacement of pentlandite–pyrrhotine by tochilinite, magnetite, and magnesite. These textures are interpreted in terms of diffusion between serpentinite matrix and the sulphide blebs.

STUDIES of disseminated opaque mineral assemblages in ultramafic rocks have, in a number of cases, led to the suggestion that the development of the opaque minerals is influenced by postmagmatic processes in the ultramafic host. Both finely disseminated nickeliferous opaque minerals, predominantly concentrated along original grain boundaries in pseudomorphic serpentinites, and larger, apparently intercumulus magmatic sulphide blebs, have been observed to vary with the nature of the alteration in the host rock (Chamberlain et al., 1965; Chamberlain, 1967; Ramdohr, 1967; Groves et al., 1974; Eckstrand, 1975; Groves and Keays, 1979). This has led to models which involve the control of opaque mineral assemblages by the chemical potentials of CO_2, O_2, and S_2 produced by alteration reactions in the volumetrically dominant host rock (Eckstrand, 1972, 1975; Groves et al., 1974).

In this paper the development of corona textures around originally magmatic interstitial iron–nickel sulphide blebs from the Mount Keith deposit, Western Australia, is interpreted in terms of diffusion

* Present address: Department of Earth Sciences, University of Leeds, Leeds LS2 9JT, UK.

between the serpentine matrix and sulphide blebs, resulting from hydration and carbonation of the original dunite. Similar corona textures developed around chrome spinels in the deposit will be discussed in a later paper.

Mount Keith. The steeply dipping sill-like ultramafic body which is the host to disseminated nickel–iron sulphides at Mount Keith, occurs in the northern part of the Agnew–Wiluna greenstone belt, in the Yilgarn block of Western Australia. The geology of the deposit has been described by Burt and Sheppy (1975) and summarized in a recent study by Groves and Keays (1979). The sill, which at Mount Keith is up to 350 m thick, is hosted by felsic metavolcanics, metabasalts and metasediments, which have been metamorphosed to mid- to upper-greenschist facies (Barrett et al., 1977). The detailed structural relationships of the intrusion are unknown, and structural duplication and multiple intrusion are possible.

The sill consists of a centrally disposed zone up to 150 m thick, of black and dark to light green serpentinites. These are bounded by grey-green serpentinites with zones of talc-carbonate, surrounded by marginal talc-carbonate rocks. Cumulate textures are well-preserved in the black serpentinites, and are less well preserved in coarsely pseudomorphic grey-green antigorite-magnesite rocks. They are progressively destroyed with the development of non-pseudomorphic antigorite in dark to light green, and some grey-green serpentinites, and are absent in talc-carbonate rocks.

Disseminated sulphides are most abundant in the black and light to dark green serpentinites, but also occur in grey-green serpentinites and talc-carbonate rocks. Evidence of the evolution of the
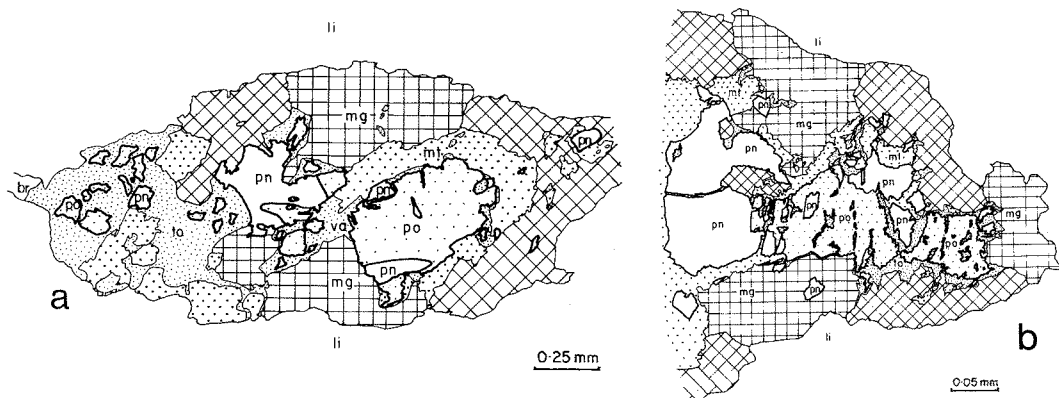
FIG. 1. Sulphide bleb textures in slightly carbonated lizardite mesh-textured black serpentinites from Mount Keith. Abbreviations are pentlandite (pn), pyrrhotine (po), tochilinite (to), magnetite (mt), magnesite (mg), and lizardite (li).

sulphide mineralogy in most green serpentinites and the talc–carbonate rocks is poorly preserved. Attention in this paper is concentrated on the sulphides in black serpentinites, because these provide the most complete evidence of the processes involved in hydration and carbonation.

Black serpentinites. The black serpentinites form a zone of variable thickness near the centre of the ultramafic body at Mount Keith. They consist of mesh-textured lizardite pseudomorphs (Wicks and Whittaker, 1977) after closely packed olivine grains 3 to 7 mm in diameter. Opaque, subrectangular mesh centres up to 2 mm in diameter consist of very finely intergrown lizardite, brucite and nickel-bearing tochilinite, surrounded by lizardite mesh rims. The mesh centre partings which represent original olivine grain boundaries, contain fine-grained brucite, magnetite, heazlewoodite, Cu-, Ni-bearing tochilinite, minor magnesite, and some antigorite laths.

Triangular cuspate opaque blebs up to 3 mm in length, form about 5 % by volume of the serpentinite, and occupy sites which were interstitial to olivine grains. These consist predominantly of pentlandite intergrown with pyrrhotine, rimmed and partly replaced by Cu-, Ni-bearing tochilinite, and surrounded by magnetite and magnesite. Fig. 1 is representative of textures developed in these blebs. The tochilinite which surrounds the sulphides partly replaces pentlandite, and extensively replaces pyrrhotine along grain boundaries and cleavages. Magnetite rims tochilinite, partly replacing it, and in places breaches the tochilinite zone to rim sulphides directly. Some magnetite appears to be surrounded by tochilinite, however it is not corroded with respect to tochilinite, and is probably contiguous with the rimming magnetite

in three dimensions. Magnesite partly to completely surrounds the magnetite zone, breaching it in places to directly rim and replace tochilinite and sulphides. The volumetrically less important chrome spinels are rimmed and partly replaced by stichtite, which is rimmed by chromian valleriite, magnetite, and magnesite.

Processes. The mineralogical evolution of the disseminated sulphide blebs which accompanies initial cooling and subsequent hydration and carbonation of the host rocks, can be considered in terms of the intensive variables, temperature and the chemical potentials (μ) of S_2, O_2 and CO_2. The discussion of the history prior to the hydration and carbonation is necessarily speculative.

Textures in unserpentinized dunites from the Agnew–Wiluna belt (Donaldson, 1981), together with sulphur isotope data (Groves and Keays, 1979), indicate that droplets of immiscible sulphide liquid were intruded with an olivine 'crystal-mush'. Crystallization of sulphide liquid during cooling produces monosulphide solid solution (*mss*) and $Ni_{3 \pm x}S_2$, leading to the formation of *mss* and pentlandite at some temperature near 600 °C (Craig, 1974). Further cooling results in exsolution from *mss*, as the lower μ_{S_2} boundary of *mss* retreats to more sulphur-rich compositions. Only below 300 °C does the complete *mss* between $Fe_{1-x}S$ and $Ni_{1-x}S$ break down, allowing the establishment of the pyrite–pentlandite tie line, and the formation of the characteristic assemblage in massive nickel sulphides, pentlandite–pyrrhotine–pyrite. The qualitative temperature–μ_{S_2} diagram, fig. 2, shows the phase relations in the Fe–Ni–S system at low temperatures. In massive nickel sulphides, the sulphide mineral assemblage buffers μ_{S_2} during cooling, path A, fig. 2. Although path A is possible
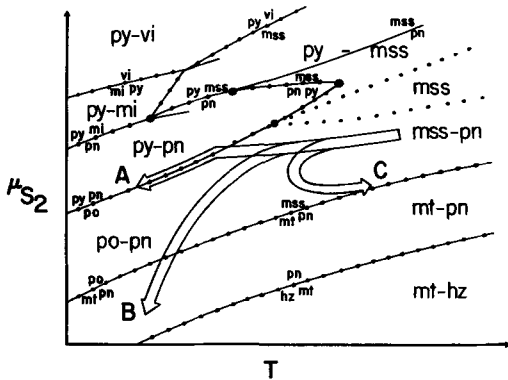
FIG. 2. Qualitative low temperature phase relations for compositions in the system Fe–Ni–S–O appropriate for nickel sulphide deposits, based on data summarized by Craig (1974). Reactions in the end-member systems Fe–S and Ni–S, and in the Ni-rich part of the system are omitted for clarity. The remaining reactions in the system are indicated by solid lines. Phase relations for a composition appropriate to disseminated nickel sulphides are given in large letters, and the phase boundaries by ornamented lines. The evolution paths are discussed in the text. Abbreviations are as in fig. 1, with the addition of monosulphide solid solution (mss), heazlewoodite (hz) and violarite (vi). Pyrrhotite (po) is used collectively for all the $Fe_{1-x}S$ structures at low temperatures.

for disseminated sulphides, if serpentinization commences before or during pyrite crystallization, the lower μ_{S_2} of the serpentinizing matrix will lower the μ_{S_2} of the sulphide blebs as indicated by path B. In this circumstance, the formation of magnetite,

heazlewoodite, or even awaruite assemblages is possible (Eckstrand, 1975).

The textures observed at Mount Keith suggest that the sulphide blebs in the original dunite consisted of pentlandite-pyrrhotite. This indicates that somewhat lower activities of μ_{S_2} than those indicated by path A were involved, although the temperature may not have decreased sufficiently for pyrite to develop, on path C, before hydration and carbonation. An explanation is required for the apparently relatively *high* μ_{S_2} conditions indicated by the presence of pentlandite-pyrrhotite at Mount Keith, in comparison with some other disseminated nickel sulphide deposits (Eckstrand, 1975). The two μ_{O_2}–μ_{S_2} diagrams, fig. 3, are for low and high μ_{MgO} respectively, during hydration at relatively low temperature. Hydration causes μ_{O_2} and μ_{S_2} to decrease (Eckstrand, 1975). Moreover, a considerable μ_{MgO} gradient exists between sulphide blebs and matrix during hydration. The response of a rock to this gradient depends on the mobility of magnesium. If Mg is immobile, the diffusion path in terms of μ_{O_2} and μ_{S_2} for the sulphide blebs is shown by path A, fig. 3a, and for the matrix by path B, fig. 3b. If, on the other hand, Mg is mobile, the path for the sulphide blebs starts as for path A, fig. 3a, but leaves that plane to go towards path B, fig. 3b. Such a path can be represented by path C, fig. 3b. The important difference between the two sulphide bleb paths is that path A avoids the tochilinite stability field. If path A is involved, the sulphide blebs can equilibrate with the matrix, and tochilinite is likely to be a minor matrix constituent. If, on the other hand, Mg is mobile, equilibration is inhibited
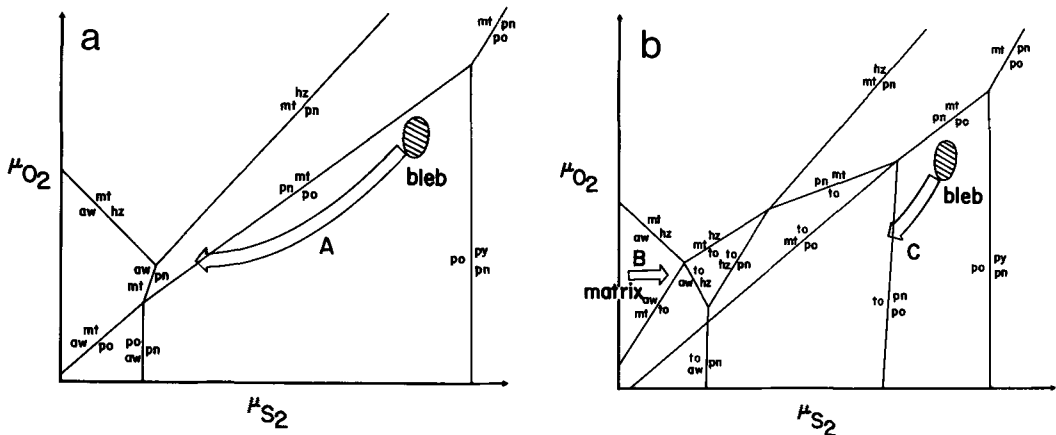

FIG. 3. Qualitative low temperature phase relations in terms of μ_{O_2}–μ_{S_2} for compositions in the system Mg–Fe–Ni–S–O at (a) low, and (b) high μ_{MgO} (after Eckstrand, 1975). Only reactions appropriate to the bulk compositions of interest are shown. The paths are discussed in the text. Abbreviations are as in fig. 2. In the construction of this diagram, tochilinite is assumed to contain some ferric iron.

because conversion of pentlandite–pyrrhotine to tochilinite occurs on the pentlandite + pyrrhotine = tochilinite reaction. In this case, tochilinite will be much more abundant, and will rim and replace the sulphide blebs, and a μ_{S_2} gradient between sulphide blebs and the matrix will survive hydration.

In summary, path A is the probable path for disseminated nickel sulphides in which tochilinite is minor or absent. In contrast, path C, which applies to the Mount Keith sulphide blebs, involves the conversion of pyrrhotine and pentlandite to tochilinite. The common occurrence of tochilinite at Mount Keith, suggests that Mg was more mobile than in deposits in which tochilinite is rare or absent, possibly due to hydration at higher temperatures.

A critical observation about the textures involving the sulphide blebs, given that they formed under the action of chemical potential gradients, is that each diffusion zone is monomineralic. This means that there is at most one component of the system which is immobile (Brady, 1976). This provides insuperable diagrammatical difficulties because of the large number of independently varying chemical potentials involved. Some success at illustrating the effects of these processes is achieved by considering these chemical potentials, three at a time, in the model system, Mg–Fe–Ni–O–S–C. Ni is considered to be the least mobile component, in the sense that its chemical potential changes passively with changes in the other chemical potentials. Fig. 4 shows the mineralogical relationships early during hydration. Brucite–magnetite–heazlewoodite, the matrix, reacts with pentlandite–pyrrhotine, the sulphide blebs. Both matrix and blebs react to form
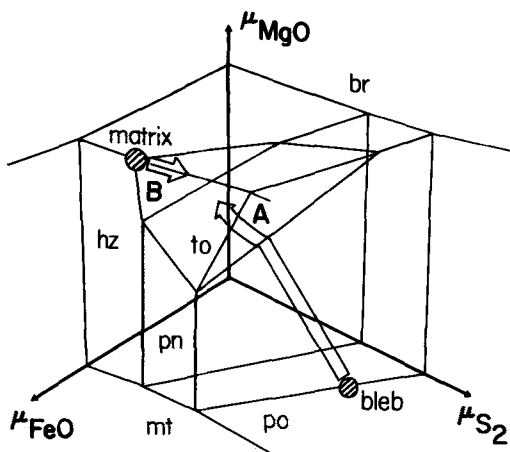
tochilinite along paths A and B, fig. 4. Note that path A involves more extensive replacement of pyrrhotine than of pentlandite by tochilinite, as observed in the textures.

A subsequent increase of μ_{O_2} in the matrix is indicated by the rimming and replacement of tochilinite by magnetite. The increase was probably due to continued influx of fluids of higher μ_{O_2}. The same reaction occurred at the outer margin of the tochilinite surrounding the sulphide blebs. Fig. 5 shows the effect of increasing μ_{O_2} conditions in the matrix, on the diffusion paths. Initially the path involves marginal replacement of tochilinite by magnetite, along path B, but when the tochilinite has been replaced, the diffusion can be represented by path C. Where the tochilinite zone is breached, magnetite replaces pentlandite and pyrrhotine. Note that heazlewoodite may remain in the matrix during this process because of the concavity of the magnetite–sulphides plane in fig. 5.
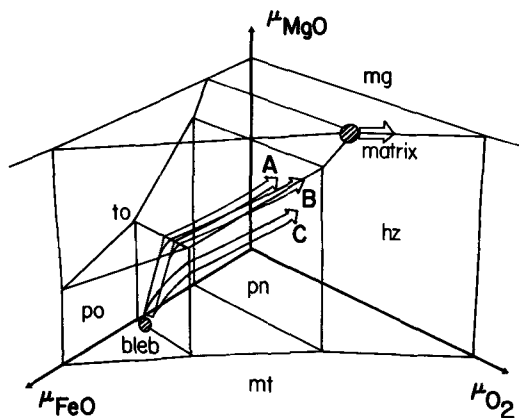

FIG. 5. A qualitative μ_{MgO}–μ_{FeO}–μ_{O_2} diagram of phase relations in the system Mg–Fe–Ni–S–O–H–C. The diffusion paths are discussed in the text. The abbreviations are as in fig. 2.

As fluid influx continued, higher μ_{CO_2} conditions were imposed on the rocks. The increased μ_{CO_2} gradient between matrix and blebs resulted in replacement of magnetite and sulphides by magnesite. Unfortunately, three dimensions are insufficient to show the appropriate phase relationships diagrammatically. In μ_{MgO}–μ_{FeO}–μ_{O_2}–μ_{CO_2} space, the matrix assemblage, magnetite–magnesite–heazlewoodite, lies on a hyperplane. By analogy with fig. 5, the concavity of the boundary planes of the magnetite and magnesite hypervolumes, means that the matrix–bleb diffusion path crosses first the magnetite, then the magnesite field, to the hyperplane. Thus the magnesite zone encroaches on

FIG. 4. A qualitative μ_{MgO}–μ_{FeO}–μ_{S_2} diagram of phase relations in the system Mg–Fe–Ni–S–O–H–C. The diffusion paths are discussed in the text. The abbreviations are as in fig. 2.

magnetite, on tochilinite, and then on pentlandite-pyrrhotine.

The minor nature of the development of non-pseudomorphic antigorite in black serpentinites is likely to be a consequence of the sealing of the fractures which allowed the infiltration of fluids during hydration and carbonation. The small amount of nucleation of antigorite in the black serpentinites would then be due to the small amount of fluid gaining access to these rocks as temperature increased to greenschist facies. In the absence of a large influx of fluid, the changes of the chemical potentials of O_2, S_2, and CO_2 would be almost entirely passive, resulting in the formation of antigorite–brucite rather than antigorite-magnesite assemblages even from originally magnesite-bearing lizardite serpentinites.

Discussion. Analysis of the sulphide textures in terms of diffusion paths on chemical potential diagrams satisfactorily explains many of the features observed in the black serpentinites at Mount Keith. Some features observed in other parts of the belt can also be explained.

At slightly higher metamorphic grade, at Betheno which is 15 km south of Mount Keith, there is evidence that magnetite which fills fractures in pentlandite and also occurs as separate grains in serpentinites, formed earlier than tochilinite. In terms of fig. 3, this implies that the μ_{O_2}–μ_{S_2} field of the bleb overlaps the pyrrhotine = pentlandite + magnetite reaction. Interaction of this bleb with the matrix involves a path down this reaction to the intersection at the boundary of the tochilinite field, where conversion of magnetite and the sulphides to tochilinite commences, instead of path C. Some magnetite does occur within the tochilinite zone of corona textures at Mount Keith; however the textures are difficult to interpret because only two-dimensional relationships can be observed and because later magnetite would have grown contiguously on earlier magnetite where the tochilinite zone is breached. If early magnetite does occur at Mount Keith, the bleb positions on figs. 4 and 5 will be displaced to higher μ_{FeO} on to the magnetite boundary; however, the consequences of the diffusion paths will be the same.

Sulphide blebs consisting entirely of pentlandite occur in barely serpentinized dunites at Betheno,

and may have occurred in the original dunites at Mount Keith. If a somewhat more Ni-rich bulk composition than that adopted in fig. 2 is considered, a one-phase pentlandite field appears across the position of the *mss* = magnetite + pentlandite reaction. In this case, path C produces mono-mineralic sulphide blebs. With reference to figs. 4 and 5, such sulphide blebs will show similar textures to the pentlandite-pyrrhotine blebs, with the bleb path starting from within the pentlandite field rather than on the pentlandite-pyrrhotine boundary. In fact, for relatively large grains of pyrrhotine and pentlandite, the diffusion paths between the matrix and each sulphide may be different, although the sequence of reaction zones will be the same. An indication of this is provided by slight differences in textures involving pentlandite and pyrrhotine, and by slight differences in tochilinite compositions in single blebs.

REFERENCES

Barrett, F. M., Binns, R. A., Groves, D. I., Marston, R. J., and McQueen, K. G. (1977) *Econ. Geol.* **72**, 1195–223.

Brady, J. B. (1976) *Geochim. Cosmochim. Acta* **41**, 113–25.

Burt, D. R. L., and Sheppy, N. R. (1975) *Austral. Inst. Mining Met. Mon.* **5**, 159–68.

Chamberlain, J. A. (1967) *Can. J. Earth Sci.* **4**, 105–53.

——McLeod, C. R., Traill, R. J., and Lachance, G. R. (1965) Ibid. **2**, 188–215.

Craig, J. R. (1974) In *Sulphide mineralogy* (P. H. Ribbe, ed.), Mineral. Soc. Am. Short Course Notes **1**.

Donaldson, M. J. (1981) *Econ. Geol.* **76**, 1698–713.

Eckstrand, O. R. (1972) *Intern. Geol. Congr., 24th Montreal, 1972*, Section 10, 25.

——(1975) *Econ. Geol.* **70**, 183–201.

Groves, D. I., Hudson, D. R., and Hack, T. B. C. (1974) Ibid. **69**, 1265–81.

——and Keays, R. R. (1979) *Can. Mineral.* **17**, 373–89.

Ramdohr, P. (1967) *Neues Jahrb. Mineral. Abh.* **107**, 241–65.

Wicks, F. J., and Whittaker, E. J. W. (1977) *Can. Mineral.* **15**, 459–88.